



## Structural investigation of mixed alkali phosphate glasses containing variable amounts of cerium oxide

A.K. Hassan<sup>1\*</sup>, A. Behairy<sup>2</sup>, M. Elhares<sup>1</sup>

<sup>1</sup>Glass Research Group, Physics Department, Faculty of Science, Mansoura University, Mansoura, 35516, Egypt

<sup>2</sup>The High Institute of Engineering and Technology, New Damietta, Egypt

Received: 28/7/2020  
Accepted: 7/8/2020

**Abstract:** In this work, several new compositions of oxides glasses in the quaternary system  $x$  CeO<sub>2</sub> replacing both sodium oxide and calcium oxide (Na<sub>2</sub>O/CaO = 1) in fixed percent (50 mol%) phosphate network forming glasses where  $x$  up to 35 mol % were successfully synthesized and investigated. The base composition of Na<sub>2</sub>O–CaO–P<sub>2</sub>O<sub>5</sub> glass corresponds to a metaphosphate category that has a structure dominated by Q<sup>2</sup> structural groups. The structural determination of the glass versus composition was studied using experimental FTIR and XRD spectral data in addition to a deconvolution analysis theoretical approach (DAT). Spectral data shows that the concentration of Ce<sub>4</sub>-O-Ce<sub>4</sub> species is increased replacing both P-O-P and P-O-Na terminal bonds. Phosphorus atoms are predominantly co-ordinated with Ce<sub>4</sub> sites as second neighbors due to a rise in CeO<sub>4</sub> species with a further rise in CeO<sub>2</sub>. FTIR spectra of CeO<sub>2</sub> containing phosphate glasses can be used to reveal the different atomic arrangements in the investigated network structure. This tool is very profound to the local symmetry, the types of chemical bonds, and other additional structural properties. The FTIR experimental results revealed that there are no differences between the structures of glasses containing up to 9 mol% CeO<sub>2</sub>. On the other, there are significant differences particularly at higher CeO<sub>2</sub> concentration. The XRD spectra revealed that there was no change in the amorphous nature of glasses up to 30 mol % CeO<sub>2</sub>. From the X-ray diffraction of cerium-rich glass, it is clear that crystalline phase formation refers to CeO<sub>4</sub>, CePO<sub>3</sub>. In such a case CeO<sub>2</sub> enters the glass network as a strong glass former species.

**Keyword:** Phosphate Glass; Cerium Oxide; FTIR, DAT

### 1. Introduction

Phosphate glasses are very interesting networks in a variety of high technology applications. These include biomaterials [1], optical devices and sealing glasses [2], nuclear waste materials [3].

The incorporation of co-oxides, e.g. Al<sub>2</sub>O<sub>3</sub> or B<sub>2</sub>O<sub>3</sub>, or rare-earth (RE) ions to the phosphate glasses is supposed to improve some cross-linking between the phosphate species through the formation of new linkages, hence increasing the strengthening of the glass network [4-6].

On the other hand, phosphate-based glasses containing Na<sup>+</sup> and Ca<sup>2+</sup> ions have useful applications in soft and hard tissue engineering, as the ions emitted from these glasses are

normal components of the human body and are thus tolerated by it (Knowles 2003) [7]. The basic building block for phosphate glasses is the PO<sub>4</sub> tetrahedral unit. These tetrahedra are bonded to three other tetrahedra through covalent bridging oxygen (BO) atoms. The addition of Na<sub>2</sub>O, CaO, ZnO and Al<sub>2</sub>O<sub>3</sub> to the P<sub>2</sub>O<sub>5</sub> glass network results in the conversion of the 3D network into a linear chain with the formation of more nonbridging oxygen atoms (NBO) at the expense of bridging oxygen atoms. Therefore, the network structure of phosphate-based glasses are composed of PO<sub>4</sub> tetrahedral that form the skeleton of the structure and metal cations that charge compensating the phosphate chains. These tetrahedra bind to form different phosphate

anions through covalent bridging oxygens. The tetrahedra is defined using  $Q^n$  terminology [8], where  $n$  represents the number of tetrahedron-bridging oxygens. Phosphate glasses can, therefore, be made with a variety of structures, from  $Q^3$  tetrahedra cross-linking network to polymer-like metaphosphate chains and  $Q^2$  tetrahedra ring to invert glasses based on small pyro- ( $Q^1$ ) and orthophosphate ( $Q^0$ ) anions, depending on the glass composition.

Several categories of phosphate glasses have been obtained depending on the  $P_2O_5$  content:

- Ultraphosphate glasses,  $P_2O_5$  content is higher than 50 mol%
- Polyphosphate glasses, (pyrophosphate and orthophosphate)  $P_2O_5$  content is lower than 50 mol% and,
- Metaphosphate glasses,  $P_2O_5$  content is equal to 50 mol%.

In these glasses, the structure and properties depend not only on the  $P_2O_5$  content but also on the charge and size of the network modifiers. Ceric oxide or cerium oxide with the chemical formula  $CeO_2$  provides the most significant source of rare earth metal cerium (RE). Ceric oxide  $CeO_2$  is the most stable phase at room temperature from which cerium may exist in two valence states as cerous (trivalent)  $Ce^{3+}$ , as well as ceric (tetravalent)  $Ce^{4+}$  ion of which  $Ce^{3+}$  is the most stable state. The two oxidation states combined with electronic transitions make cerium an important material for various applications and the principal interests to study the structure and properties of cerium containing modified phosphate glass in this paper.

Previous studies [9-11] have indicated that the incorporation of cerium oxide concentration is well limited in phosphate glasses because of the so-called concentration quenching and the presence of rare earth clustering. Modifying metaphosphate glasses, based on  $P_2O_5$  as the glass network former and CaO and  $Na_2O$  as network modifiers are suitable for accommodation of large proportions of rare-earth ions compared to other glass systems.

Some earlier investigations were carried out on rare-earth-doped phosphate glasses [12, 13] but no studies have been reported on mixed alkali metaphosphate glasses containing  $CeO_2$ .

Thus it was of some importance to measure and investigate infrared absorption spectra to study the effect of  $CeO_2$ 's introduction into mixed alkali metaphosphate glasses that can provide some knowledge about microstructural changes occurring in the glass.

In the present paper, a depth study of the effect of cerium addition into the phosphate glass network in mixed alkali metaphosphate glasses of general composition  $xCeO_2:(50-x)Na_2O+CaO:50P_2O_5$  glasses in which  $Ce_2O$  oxide content was varied in the range ( $0 \leq x \leq 35$  mol %). The results enable us to discuss the changes in the network structure of phosphate glasses upon the addition of ceria in considerable details, indicating different structural modifications on short-range order for ceria-rich glasses. Therefore, it will be possible to obtain complementary views on the atomic environments and get new structural insights into the local coordination of the rare-earth ions ( $CeO_2$ ) as well as of the amorphous network that constitutes their host environment.

## Material and Methods

### 2. Glass preparation and characterizations

#### 2.1. $CeO_2$ modified phosphate glasses

The phosphate glass series presented in this study followed the general fabrication procedure and are prepared from appropriate amounts of chemically pure reagent-grade raw materials. Rare earth oxide ( $CeO_2$ ) was supplied by Sigma Aldrich which used in as received condition without any further purification (as AnalaR  $CeO_2$ ).  $Na_2O$  and CaO have been introduced as their respective anhydrous carbonates while  $P_2O_5$  has been added as ammonium dihydrogen phosphate ( $NH_4H_2PO_4$ ). The phosphate glasses under investigation have the chemical composition according to the system  $xCeO_2-(50-x)Na_2O+CaO-50P_2O_5$  glasses ( $0 \leq x \leq 35$  mol %). A batch size of about 50 g was used. The weighed batches were mixed and melted in porcelain crucibles (50 CC) in a high-temperature furnace for 20 minutes at about 1400 °C, depending on composition. All glass samples were melted in ordinary atmospheric conditions and rotated occasionally to promote complete mixing and homogeneity. Once a melt had formed, it was poured into a preheated stainless steel molds, and air quenched with

natural cooling gradually down to room temperature. The prepared glasses were clear, colorless, and bubble-free. All of the glass samples were placed in a desiccator to prevent potential moisture attacks before use. All the glass compositions were obtained in an amorphous state, as evidenced by experiments in powder X-ray diffraction.

## 2.2. X-ray Diffraction Measurements

XRD experiments were conducted for fine glass powdered samples to get an idea of the structure and to examine the amorphous state of the prepared glasses. X-ray diffraction pattern was performed on a Bruker Axs-D8 system using  $\text{CuK}_\alpha$  radiation ( $\lambda_{\text{CuK}_\alpha} = 0.1540600 \text{ nm}$ ) in the  $2\theta$  diffraction angle range between  $4^\circ$  -  $80^\circ$ . The obtained data was steeply accumulated with  $0.02^\circ$  intervals fitted using Joint Committee on Powder Diffraction and Standards (JCDPS). The X-Ray tube operated at 40kV potential and 30 mA current.

## 2.3. Infrared absorption measurements

IR spectrum measurements of glasses between  $400 \text{ cm}^{-1}$  and  $4000 \text{ cm}^{-1}$  were obtained using an FTIR spectrometer (type Mattson 5000) with a resolution of  $2 \text{ cm}^{-1}$  at room temperature. Infrared absorption spectra were performed immediately after preparation to prevent water moisture attack. Pulverized powdered glassy samples were mixed using the standard method for potassium bromide (KBr) pellets with a fixed ratio 1:100 and the mixture was implemented to a constant pressure of  $5 \text{ ton/cm}^2$ . The pulverized sample pellet spectrum recorded has been subtracted from that of the KBr matrix.

## Microstructural Analysis

A quantitative analysis was performed for the infrared spectrum through accurate deconvolution of the absorbance profiles using the [Peak Fit 4.12 program] computer program. The program was designed to define hidden peaks using numerical iterative methods and suitable peak definitions including height, intensity, and full width at half maximum (FWHM) and other remind factors that control the quality of the fitting process. The program was supplied by Jandel scientific co., copyright© 2003 AISN Software.)

The fitting process was performed on a normalized data corrected for background (using two-points baseline regime) and dark current noises. Spectroscopic acceptable line shapes usually Gaussian ones were used for the fitting process. FWHM, intensity, position, and area of each band are automatically adjusted within the programed route based on the minimization of the differences between simulated spectrum and experimental data.

## 3. Results and Discussion

In this work several new compositions of oxides glasses in the quaternary system  $x\text{CeO}_2$ - $(50-x)\text{Na}_2\text{O}+\text{CaO}-50\text{P}_2\text{O}_5$  glasses ( $0 \leq x \leq 35 \text{ mol } \%$ ) were investigated. The glasses have a fixed  $\text{P}_2\text{O}_5$  content at 50 mol% and the  $\text{Na}_2\text{O}:\text{CaO}$  ratio was one. The base composition of  $\text{Na}_2\text{O}-\text{CaO}-\text{P}_2\text{O}_5$  glass corresponds to a metaphosphate category that has a structure dominated by  $\text{Q}^2$  groups. The structural determination of the glass versus composition was investigated via experimental and deconvolution analysis technique (DAT) FTIR spectroscopic techniques. The study of FTIR spectra of  $\text{CeO}_2$  containing phosphate glasses can be used to reveal the different atomic arrangements in the investigated network structure. These tools are very sensitive to the local symmetry, chemical bond types, and other additional structural characteristics. The FTIR experimental results revealed that there are no differences between the structure of glasses containing up to 9 mol%  $\text{CeO}_2$ . On the other, there are significant differences particularly, at higher  $\text{CeO}_2$  concentrations.

### 3.1. FTIR Absorption Spectra

It was known that the gradual addition of modifier oxide to phosphate network leads to subsequent changes in the phosphate units from a high cross-linking  $\text{Q}^3$  structure to a chain-like  $\text{Q}^2$  network, to  $\text{Q}^1 / \text{Q}^0$  depolymerized glasses. The basic structural unit of vitreous  $\text{P}_2\text{O}_5$  is  $\text{PO}_4$  tetrahedral units forming primarily three-dimensional (3D) network with structural unit form  $\text{Q}^3$  [7,9]. Adding a modifier will depolymerize part of the 3D network, and simultaneously form a 2D chain structure (structural units of  $\text{Q}^2$ ). NMR details of currently available glasses which contain 50 mol % modifier oxide ( $\text{Na}_2\text{O}$  and  $\text{CaO}$ ) indicated that, chain structure created by  $\text{Q}^2$

units is dominated species in the network of the investigated glass.

The phosphate glass networks are categorized according to the oxygen-to-phosphorus ratio O/P, which defines the degree of polymerization of the P-O-P network or neighboring P-tetrahedra connections via bridging oxygen (BOs), and so dominating  $Q^n$  species shown in Figure (1)[14]. Table 1

describes the various forms of O / P based phosphate glass networks.

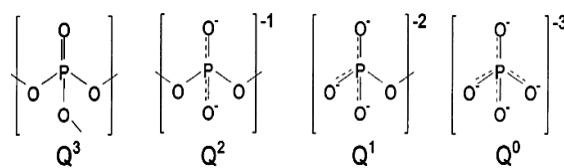


**Figure (1)** Schematic diagram of tetrahedral phosphate sites that may be present in phosphate glasses.

**Table 1:** Ranges of the composition of phosphate glass and classification of glass networks according to  $M_2O/P_2O_5$  and O/P ratios and  $Q^n$  species [15-17].

Phosphate Network	Vitrous $P_2O_5$	Ultraposphate	Metaphosphate $PO_3^-$	Polyphosphate	Polyphosphate	
					Pyrophosphates $P_2O_7^{4-}$	Orthophosphate $PO_4^{3-}$
$M_2O/P_2O_5$	0		1		2	3
Ratio O/P	2.5	< 3.0	3.0	3.0 >	3.5	4.0
$Q^n$ species	$Q^3$	$Q^3 + Q^2$	$Q^2$	$Q^2 + Q^1$	$Q^1$	$Q^0$

### Spectral Assignments

It has been shown that the phosphate tetrahedron ( $PO_4^{3-}$ ) exists in all  $P_2O_5$  glasses [18] and has two basic vibrational frequencies at approximately 1100 and 980  $cm^{-1}$ . The latter two vibration frequencies are observed even in the Raman spectra. The 1100  $cm^{-1}$  band has also been identified and assigned to stretching vibrations of non-bridging P-O<sup>-</sup> bonds [19]. It is understood that a P = O unit exists in any member of the  $RO-P_2O_5$  family of glasses with R= Li, Na, Ag and Pb. The suggested range for this band is between 1200  $cm^{-1}$  and 1500  $cm^{-1}$ . Miller and Wilkins [20] took the view that the  $(PO_4)^{3-}$  ion exhibits normal vibrations in the 1100-1040  $cm^{-1}$  region. The P = O and P-O<sup>-</sup> groups, respectively, produce characteristic vibrational bands at 1282  $cm^{-1}$  and 1205  $cm^{-1}$ . Bartholomew [21] and references in his article has analyzed the IR spectra of sodium recta-phosphate [ $Na_2P_2O_6$ ] glasses and silver recta-phosphate [ $Ag_2P_2O_6$ ] glasses and found a difference in band positions of P= O and P-O<sup>-</sup> in silver glasses relative to sodium glass positions. This difference may be connected with the ionic field strength of the modifier ion.

The analysis of vibrational spectra of modified phosphate glasses containing  $CeO_2$  is treated in terms of vibration of terminal ( $PO_2$ ) and ( $PO_3$ ) units and oxygen bridges (P-O-P) rather than in terms of polyhedra. FTIR spectra of present phosphate glasses containing different concentrations from  $CeO_2$  with a frequency range from 400 to 1600  $cm^{-1}$  are

illustrated in figure 2. Spectra were examined to determine the relative intensity of the IR bands which are responsible for the various phosphate groups. It can be seen from this figure that there are some differences in spectral features between cerium free and cerium containing phosphate glasses. It has been observed in present investigated glasses that there is no change in spectral feature with changing  $CeO_2$  concentration between 0 and 9 mol %, since there is no detectable shift in both peak area and position. These can be attributed to the presence of the same structural units in the phosphate network even upon changing  $CeO_2$  concentration.

On the other hand, overlapping between FTIR spectral bands is the main character observed in all glasses containing  $CeO_2$  particularly in the region of (800-1200  $cm^{-1}$ ). The absorption spectra of these glasses seem to consist of relatively broad bands that may reflect the structural disorder of the different phosphate structural groups. It is observed that there are some changes in the spectral feature of glasses containing a higher  $CeO_2$  concentration > 9 mol %. From Figure 2 and Table 2 it can observe that:

as  $CeO_2$  is increased the most noticeable change in the IR spectra is the gradual shift of a  $\nu_{as}(PO_2)$  band towards smaller wave numbers accompanied by intensity decrease and tends to broaden. The peak around the highest wavenumber i.e. in the range of 1280-1248  $cm^{-1}$  is related to the  $PO_2$  and P= O

stretching mode of the tetrahedral phosphate and its intensity depends heavily on the content of CeO<sub>2</sub>. This band decreases both in area and intensity due to the addition of cerium which indicates the decrease in non-bridging oxygen in phosphate matrix upon the presence of CeO<sub>2</sub> as shown in Figure 1. As a result, the band intensity and area centered at approximately 1280 cm<sup>-1</sup>, attributable to the absorption of P=O and NBO in (PO<sub>2</sub>) Q<sup>2</sup> chains [14] are both reduced as the content of CeO<sub>2</sub> increases. This leads to a reduction of the long-chain, and therefore the phosphate glass structure is composed of a shorter chain of Q<sup>2</sup> structural units [22-24].

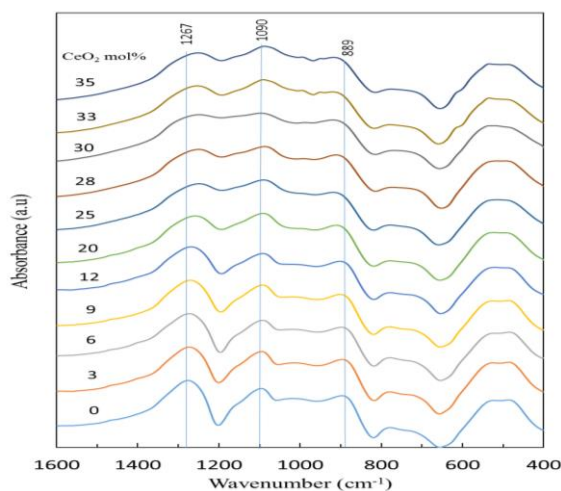


**Figure (2)** FTIR absorption spectra of studied glasses containing a variable amount of cerium

**Table 2:** The observed dominant bands of IR spectra in cerium modified phosphate glasses and their assignments [14, 22-30].

Wavenumber (cm <sup>-1</sup> )	Attributions
~400-650	deformation modes of bending vibration of P-O <sup>-</sup> groups
~ 730	(P-O-P) symmetric stretching mode of bridging oxygen (BO) Q <sup>2</sup> .
~ 770	(P-O-P) symmetric stretch (BO) Q <sup>1</sup> .
~ 900-920	Symmetric and asymmetric stretches of P-O-P bridges
~ 900	(PO <sub>4</sub> ) symmetric stretch (NBO) Q <sup>0</sup> .
~ 950-1060	P-O <sup>-</sup> stretch Q <sup>0</sup> chain terminator.
~ 1100	(P-O) symmetric stretch (NBO) Q <sup>1</sup> .
~1080-1140	P-O <sup>-</sup> (NBO) stretching, Q <sup>1</sup> chain terminator.
~1160	(PO <sub>2</sub> ) symmetric stretching (NBO) Q <sup>2</sup> .
~1248-1280	Vibrational mode P=O superposed with PO <sub>2</sub> asymmetric stretching vibration band in Q <sup>2</sup> units.

The broad hump lies between 800-1200 cm<sup>-1</sup> in the region becomes narrower and contains sharper envelopes for cerium-rich glasses (33-35 mol %), which may imply mixed P-O-Ce

bonds formation. It may result in an increased concentration of Q<sup>2</sup> and Q<sup>3</sup> units [14, 23]. The area and intensity of the 620-830 cm<sup>-1</sup> wide band have shown decreasing trends in the region. It refers to the stretching vibration of oxygen atoms in P-O-P bridges [24, 25]. This band's decreasing area results in a decrease in the bridging oxygen concentration linked between two phosphorous ions. These results in an increase of Ce-O-P bonds in phosphate network which is obvious in glasses containing > 9 mol % CeO<sub>2</sub>. In such a case, the peak between 620 cm<sup>-1</sup> and 830 cm<sup>-1</sup> re-increased again.

The absorption band around 1100 cm<sup>-1</sup> is assigned to mixed vibration of Q<sup>1</sup> and Q<sup>2</sup> [26-28] type of bonding in the phosphate tetrahedral containing 3 and 2NBO. The shape of this band differs from that of cerium free glass. Peaks at about 900 cm<sup>-1</sup> and 1100 cm<sup>-1</sup> are assigned to groups of PO<sub>4</sub> with both Q<sup>0</sup> and Q<sup>1</sup>. The feature around 1020 cm<sup>-1</sup> is corresponding to the symmetric stretching mode of the Q<sup>0</sup> type of linkage and this absorption band also decreases with CeO<sub>2</sub> substitution at the expense of (Ca<sup>2+</sup> + Na<sup>+</sup>) modifier. This species Q<sup>0</sup> acts as the mode of chain terminator corresponds to the structure of the orthophosphate. The shoulder at about 1160 cm<sup>-1</sup> which seems to be decreasing in intensity with increased CeO<sub>2</sub> content is attributed (PO<sub>2</sub>) symmetric stretching with (NBO) in Q<sup>2</sup>, suggested polymerization of the glass network due to the addition of CeO<sub>2</sub>. Then from the above discussion, it can conclude that substitution of (Ca<sup>2+</sup>+Na<sup>+</sup>) with CeO<sub>2</sub> will result in decreasing NBO which formed in phosphate network. When the concentration of CeO<sub>2</sub> reaches 30 % there are additional new small envelopes at about 630 cm<sup>-1</sup> and between 950 cm<sup>-1</sup> and 1020 cm<sup>-1</sup>.

The 1100 cm<sup>-1</sup> band and the shoulder at about 1160 cm<sup>-1</sup> were assigned to a symmetrical out- of chain stretching vibration of PO<sub>2</sub> groups (i.e. phosphorus with two non-bridging oxygens). Symmetric and asymmetric stretches of P-O-P bridges give rise to the 920-900 cm<sup>-1</sup> and 770 cm<sup>-1</sup> bands. The intense bands below 600 cm<sup>-1</sup> should be attributed to deformation modes of bending vibration of P-O<sup>-</sup> groups [29, 30].

Studies of the effect of CeO<sub>2</sub> on phosphate glasses [29, 30] generally accepted that the cerium's role was to act as a network modifier. To understand the structure-property correlations of cerium-containing glasses remains limited, in particular for the complex multi-component system.

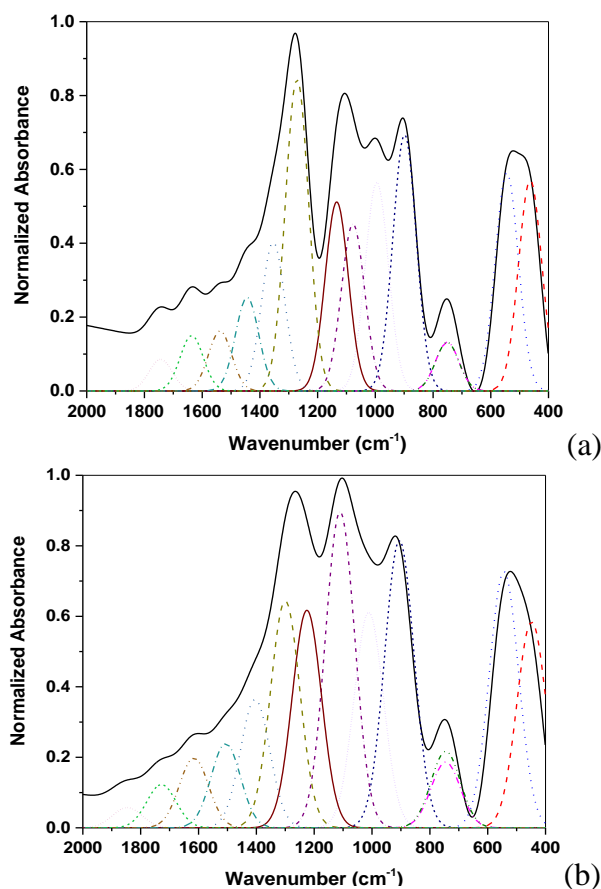
It was found that CeO<sub>2</sub> enters the glass as a glass modifier by breaking the P-O-P bonds and may introduce coordination defects in the studied CeO<sub>2</sub> glasses of less than 9 mol % along with NBO atoms. This leads to a lowering of the long-chain, and thus the construction of P<sub>2</sub>O<sub>5</sub> glasses would require a shorter Q<sup>2</sup> chain.

Deconvoluted data shows that the nonbridging absorbance spectrum areas in Q<sup>2</sup> stretching mode (Ca 1280 cm<sup>-1</sup>) decrease when the CeO<sub>2</sub> content increases to a minimum of 35 mol % of CeO<sub>2</sub>. Such decreasing behavior will result in progressive polymerization of the phosphate network, and also an increase in the average bond length of the band of P-nonbridging oxygen around 1160 cm<sup>-1</sup>. This behavior has shown a few increments with an increasing concentration of CeO<sub>2</sub> in Q<sup>3</sup> species. By introducing more CeO<sub>4</sub> units into the structure of the glass and their ability to shield and organize with PO<sub>4</sub> units, such a tendency is possible towards CeO<sub>2</sub>'s major role. As a result, the rise in CeO<sub>2</sub> content leads to an increase of Ce<sub>4</sub>-O-Ce<sub>4</sub> bonds at the expense of P-O-P. In such a situation, the glass structure consists primarily of bond Ce<sub>4</sub>-O in groups of CeO<sub>4</sub>. There may also be suggestions for the creation of certain Ce<sub>4</sub>-O mixed vibrations with P-O. The findings of these measurements are quite in line with those of the same glass obtained from the NMR. Figures (3.a, b) reveals exemplified deconvoluted data for two samples, (a) base glass that does not contain cerium oxide, (b) samples that contain 20 mol% of cerium oxide.

Depolymerization of the network enhanced linkage through charge compensation, and improved compactness due to close packing is suggested as the cause of the existence of CeO<sub>2</sub> content. This suggests that the network has a high degree of cross-linkage between the PO<sub>4</sub> units, mediated by the incorporated rare-earth ions. This high level of cross-linkage could play a significant part in the observed increased

resistance to hygroscopic attack displayed by these glasses over other phosphate systems.

Moreover, the link between CeO<sub>4</sub> and the different phosphate groups within the glass network is the most abundant. Such an argument becomes obvious from FTIR spectra, especially in glasses containing more than 30 mol % CeO<sub>2</sub>, where the shoulder is assigned a Ce-O vibration at approximately 630 cm<sup>-1</sup> in a phase rich of cerium phosphate mixed units. The findings provide some important insights into the phosphate-based glass structure and suggest its suitability for further research to develop future biomedical applications of these glasses



**Figures (3)** Exemplified deconvoluted data for two samples, (a) base glass that does not contain cerium oxide, (b) samples that contain 20 mol% of cerium oxide.

### 3.2. X-ray diffraction analysis

Different observations are raised from the XRD spectra of glass containing CeO<sub>2</sub> when comparing it with that of glass free from it. The x-ray diffraction examinations were performed to get an idea about the structure and to investigate the amorphous state of the prepared glasses. Since powder XRD analysis is a very

useful technique and becomes important for the crystallinity structure of glasses. X-ray diffraction patterns for the glasses up to 25 mol% CeO<sub>2</sub> showed no sharp peaks but exhibit a broad hump as illustrated in figure 4 which is the characteristic of the glassy nature of the samples. There is no improvement in the XRD spectra that indicated that even after CeO<sub>2</sub> additions glasses remained amorphous. The amorphous character of the samples indicates that homogeneous glasses have been obtained.

At higher CeO<sub>2</sub> content (>25 mol%), we notice the presence of some little diffraction lines which may lead to the formation of some ordered micro-domain in the samples (Figure 4). This means that the crystallization of the glass was just starting. Here there is a transition from amorphous character to some crystalline phases occurred showing the existence of many oxide phases. The change in behavior can be attributed to the cross-linking of Ce cations between phosphate chains which strengthened the glass network. Increasing CeO<sub>2</sub> content up to 35 mol% leads to shortening of phosphate chains as suggested above.

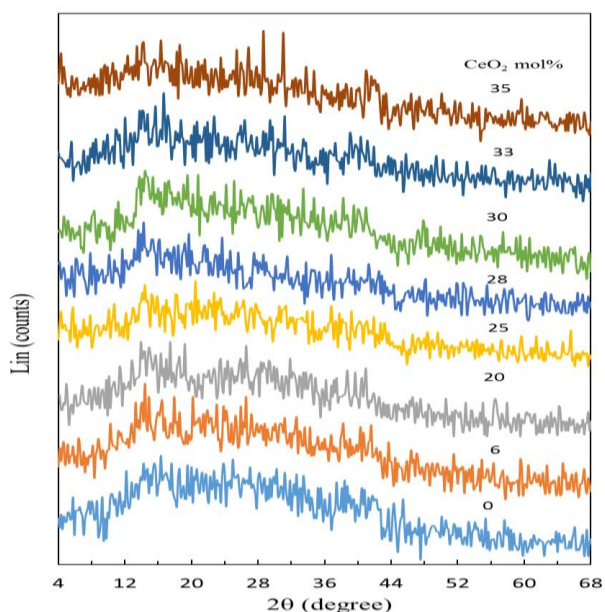


**Figure (4)** XRD pattern of modified phosphate glasses containing different concentrations of CeO<sub>2</sub>.

#### Conclusion

The glass compositions  $x\text{CeO}_2-(50-x)\text{Na}_2\text{O}+\text{CaO}-50\text{P}_2\text{O}_5$  were prepared and the effect of Ce<sub>2</sub>O substitution by (Na<sub>2</sub>O+CaO) on their structural characteristics was studied. For the first time, the structure of glasses in the modified cerium phosphate system has been

explored by the correlation of results obtained from XRD and FTIR analysis. FTIR absorbance analysis has confirmed that the rate of producing non-bridging bonds in phosphate groups is reduced upon CeO<sub>2</sub> addition. The concentration of Ce<sub>4</sub>-O-Ce<sub>4</sub> species is increased at the expense of both P-O-P and P-O Na terminal bonds. The phosphorus atoms are primarily coordinated with Ce<sub>4</sub> sites as second neighbors leading to an increase in CeO<sub>4</sub> species with a further increase in the concentration of CeO<sub>2</sub>. An increased fraction of Q<sup>3</sup> is considered in the phosphate network due to the development of structural species of CeO<sub>4</sub>. XRD pattern confirms the formation of the glassy phase enriched with Ce ceria-rich glass. From the X-ray diffraction of cerium-rich glass, it is clear that crystalline phase formation refers to CeO<sub>4</sub>, CePO<sub>3</sub>. In such a case CeO<sub>2</sub> enters the network of glass as a former species of strong glass.

#### 4. References

1. Vogel, W., Hoeland, W., Naumann, K., & Gummel, J. (1986). Development of machineable bioactive glass ceramics for medical uses. *Journal of non-crystalline solids*, **80(1-3)**, 34-51.
2. Wilder Jr, J. A. (1980). Glasses and glass ceramics for sealing to aluminum alloys. *Journal of Non-Crystalline Solids*, **38**, 879-884.
3. Donald, I. W., & Metcalfe, B. L. (2004). Thermal properties and crystallization kinetics of a sodium aluminophosphate based glass. *Journal of non-crystalline solids*, **348**, 118-122.
4. Kreidl, N. J., & Weyl, W. A. (1941). Phosphates in ceramic ware: IV, phosphate glasses. *Journal of the American Ceramic Society*, **24(11)**, 372-378.
5. Brow, R. K. (1993). Nature of alumina in phosphate glass: I, properties of sodium aluminophosphate glass. *Journal of the American Ceramic Society*, **76(4)**, 913-918.
6. Brow, R. K. (2000). The structure of simple phosphate glasses. *Journal of Non-Crystalline Solids*, **263**, 1-28.
7. Knowles, J. C. (2003). Phosphate based glasses for biomedical applications.

- Journal of Materials Chemistry*, **13(10)**, 2395-2401.
8. Liebau, F. R. I. E. D. R. I. C. H. (1981). The influence of cation properties on the conformation of silicate and phosphate anions. Structure and bonding in crystals, **2**, 197-232.
  9. Brow, R. K., Click, C. A., & Alam, T. M. (2000). Modifier coordination and phosphate glass networks. *Journal of non-crystalline solids*, **274(1-3)**, 9-16.
  10. Du, J., Kokou, L., Rygel, J. L., Chen, Y., Pantano, C. G., Woodman, R., & Belcher, J. (2011). Structure of cerium phosphate glasses: molecular dynamics simulation. *Journal of the American Ceramic Society*, **94(8)**, 2393-2401.
  11. Mountjoy, G. (2007). Molecular dynamics, diffraction and EXAFS of rare earth phosphate glasses compared with predictions based on bond valence. *Journal of non-crystalline solids*, **353(18-21)**, 2029-2034.
  12. Harani, R., Hogarth, C. A., Ahmed, M. M., & Morris, D. F. C. (1984). Optical absorption spectra of praseodymium phosphate glasses. *Journal of Materials Science Letters*, **3(9)**, 843-844.
  13. Ahmed, M. M., Harani, R., & Hogarth, C. A. (1984). The optical energy gap in praseodymium phosphate glasses. *Journal of materials science letters*, **3(12)**, 1055-1057.
  14. Abdelghany, A. M. "Modeling, (2015): structural, and spectroscopic studies of cobalt-doped lithium phosphate glasses and effect of gamma irradiation." *Spectroscopy Letters* **48.9** 623-630.
  15. Brow, R. K. (2000). the structure of simple phosphate glasses. *Journal of Non-Crystalline Solids*, **263**, 1-28.
  16. Suzuya, K., Price, D. L., Loong, C. K., & Martin, S. W. (1998). Structure of vitreous P<sub>2</sub>O<sub>5</sub> and alkali phosphate glasses. *Journal of non-crystalline solids*, **232**, 650-657.
  17. Hoppe, U. (1996). A structural model for phosphate glasses. *Journal of Non-Crystalline Solids*, **195(1-2)**, 138-147.
  18. Corbridge, D. E. C., & Lowe, E. J. (1954). The infra-red spectra of inorganic phosphorus compounds. Part II. Some salts of phosphorus oxy-acids. *Journal of the Chemical Society (Resumed)*, **0**, 4555-4564.
  19. Paul, A. (1989). *Chemistry of glasses*. Springer Science & Business Media.
  20. Miller, F. A., & Wilkins, C. H. (1952). Infrared spectra and characteristic frequencies of inorganic ions. *Analytical chemistry*, **24(8)**, 1253-1294.
  21. Bartholomew, R. F. (1972). Structure and properties of silver phosphate glasses—Infrared and visible spectra. *Journal of Non-Crystalline Solids*, **7(3)**, 221-235.
  22. Hammad, A. H., & Abdelghany, A. M. (2016). Optical and structural investigations of zinc phosphate glasses containing vanadium ions. *Journal of Non-Crystalline Solids*, **433**, 14-19.
  23. Gresch, R., Müller-Warmuth, W., & Dutz, H. (1976). <sup>11</sup>B and <sup>27</sup>Al NMR studies of glasses in the system Na<sub>2</sub>O-B<sub>2</sub>O<sub>3</sub>-Al<sub>2</sub>O<sub>3</sub> ("NABAL"). *Journal of Non-Crystalline Solids*, **21(1)**, 31-40.
  24. Shih, P. Y., Yung, S. W., & Chin, T. S. (1999). FTIR and XPS studies of P<sub>2</sub>O<sub>5</sub>-Na<sub>2</sub>O-CuO glasses. *Journal of non-crystalline solids*, **244(2-3)**, 211-222.
  25. Lai, Y. M., Liang, X. F., Yang, S. Y., Wang, J. X., Cao, L. H., & Dai, B. (2011). Raman and FTIR spectra of iron phosphate glasses containing cerium. *Journal of Molecular Structure*, **992(1-3)**, 84-88.
  26. Du, J., Kokou, L., Rygel, J. L., Chen, Y., Pantano, C. G., Woodman, R., & Belcher, J. (2011). Structure of cerium phosphate glasses: molecular dynamics simulation. *Journal of the American Ceramic Society*, **94(8)**, 2393-2401.
  27. El-Damrawi, G., & El-Egili, K. (2001). Characterization of novel CeO<sub>2</sub>-B<sub>2</sub>O<sub>3</sub> glasses, structure and properties. *Physica B: Condensed Matter*, **299(1-2)**, 180-186.
  28. Marzouk, M. A., ElBatal, H. A., & Abdelghany, A. M. (2018). Gamma irradiation effect on structural and spectral properties of CeO<sub>2</sub>, Nd<sub>2</sub>O<sub>3</sub>, Gd<sub>2</sub>O<sub>3</sub>, or Dy<sub>2</sub>O<sub>3</sub>-doped strontium borate glass. *Silicon*, **10(1)**, 29-37.
  29. Ivanova, Y. Y., Spassova, E. J., Kashchieva, E. P., Bursukova, M. A., & Dimitriev, Y. B. (1995). Structure of gel materials in the system Ce<sub>2</sub>O<sub>3</sub>-Al<sub>2</sub>O<sub>3</sub>-



- $P_2O_5$ . *Journal of non-crystalline solids*, **192**, 674-678.
30. ElBatal, H. A., Abdelghany, A. M., ElBatal, F. H., ElBadry, K. M., & Moustaffa, F. A. (2011). UV-visible and infrared absorption spectra of gamma irradiated CuO-doped lithium phosphate, lead phosphate and zinc phosphate glasses: a comparative study. *Physica B: Condensed Matter*, **406(19)**, 3694-3703.